Unsteady Supersonic Flow Calculations for Wing-Body Combinations Using Harmonic Gradient Method

Pablo Garcia-Fogeda*
Arizona State University, Tempe, Arizona
P. C. Chen†
Zona Technology, Inc., Mesa, Arizona
and
D. D. Liu‡
Arizona State University, Tempe, Arizona

The Harmonic Gradient Method (HGM) developed for nonplanar wings in unsteady supersonic flow is generalized to include asymmetric bodies and wing-body combinations. The H-G model is incorporated with a newly developed Bundled Triplet Method (BTM) for treatment of arbitrary bodies. The present method is an effective one in handling unsteady wing-body interference. In particular, the BTM has proven to be computationally more efficient than the surface panel method. Numerical studies for various configurations include: pressures on asymmetric conical bodies, generalized forces on cylindrical panels and stability derivatives for bodies and wing-body combinations. All computed results are in good agreement with existing theoretical results and measured data.

Introduction

In recent years, there has been much effort toward developing effective methods for nonplanar lifting surfaces in unsteady supersonic flow.[1-5] Most of these investigators followed the Potential Gradient Method (PGM) approach and modified it further. By contrast, the Harmonic Potential Gradient Method (HGM, Ref. 6) developed recently encompasses a more general formulation by which it also achieves the computation accuracy and effectiveness.

On the other hand, current demands in design and performance also call for an effective prediction method for wing-body configurations. Hence, a natural step is to extend the HGM for wing-body combinations. In practice, the unsteady wing-body aerodynamics is of primary importance for supersonic aeroelastic applications. To continue the HGM development, we have, therefore, generalized the method for treatment of axisymmetric bodies in oscillation with flexure.[7-9] Although these efforts would serve as necessary building blocks for an integrated wing-body program, its general formulation is hardly straightforward. In so doing, the unsteady supersonic formulation for asymmetric bodies must be resolved first in order to bridge through the wing aerodynamics to the one for wing-body. Such an approach in steady flow is attributed to Wards,[10] Nielsen,[11] and Woodward,[12] among others.

We have extended Wards' vortex multiplets approach to a collocation method, using a line-singularity approach for supersonic computations of asymmetric bodies.[13] Our experience showed, however, that the extended method yields acceptable results for bodies of mildly asymmetric cross sections but not for highly irregular ones. To improve the accuracy of the latter, more collocation points must be added on the body. Unfortunately, this will introduce a set of kernel functions related to higher order singularities. In turn, this will enhance the difficulty in the evaluation of the aerodynamic influence coefficients (AIC) matrix.

Woodward extended von Karman's line singularity method[14,15] to a line/surface panel method in which the surface elements on the body will account for the wing-body interference. Woodward later abandoned this method due to its cumbersome procedure and adopted the all-surface panel method instead.

Although Woodward's work (USSAERO) has claimed much success, its extension to unsteady flow is by no means obvious. Perhaps the only unsteady work following this line was that of Morino et al.,[16] in which few unsteady results were made available. The basic difficulty in applying the surface panel method to bodies lies in the complications in the geometrical problem due to Mach cone-body interaction, coupled with unsteady kernel function evaluations.

To circumvent these difficulties, we have now developed a new method using a bundle of combined low-order singularities (sources and doublets only) for general treatments of asymmetric bodies of arbitrary shapes, including slope discontinuities. This method is named "bundled triplet method" (BTM). When combined with HGM, it will be seen that BTM can be applied to wing-body combinations effectively for unsteady supersonic computations.

The objective of this paper is, therefore, to present this combined method and its applications. For verification, numerical examples will be given in terms of unsteady pressures and stability derivatives for asymmetric bodies and wing-body combinations in oscillation and generalized forces for vibrating cylindrical panels.

In what follows, length and vorticity variables are nondimensionalized by the referenced length L and the freestream velocity U_∞, respectively.

Formulation for General Bodies

Following the formulation in Ref. 8, a body-fixed coordinate system chosen requires that the x-axis remains to be the body axis at all times. For bodies in harmonic motions, the

Presented as Paper 88-0568 at the AIAA 26th Aerospace Sciences Meeting, Reno, NV, Jan. 11-14, 1988; received Feb. 23, 1988; revision received Jan. 20, 1989.

*Faculty Associate, Mechanical and Aerospace Engineering; currently Assistant Professor, Ciudad Universitaria, Madrid, Spain. Member AIAA.

†Graduate Student; currently President, Zona Technology. Member AIAA.

‡Associate Professor, Mechanical and Aerospace Engineering. Member AIAA.

total velocity potential Ω can be expressed as

$$\Omega(x,r,\theta,t) = x + \delta_0 e^{ikt} g'(x) r\cos\theta + \phi_0(x,r,\theta) + \delta_0 e^{ikt}\phi_1(x,r,\theta) \tag{1}$$

where δ_0 is the amplitude of oscillations, k the reduced frequency, $k = \omega L/U_\infty$, ω the circular frequency, and $g(x)$ the normalized bending mode function; ϕ_0 is the perturbed potential due to steady mean flow and ϕ_1 due to unsteady crossflow.

It can be shown that the governing equations for ϕ_0 and ϕ_1 are the linearized equations and the first-order equation, respectively, i.e.:

$$(1 - M_\infty^2)\phi_{\sigma xx} + \phi_{\sigma rr} + \frac{1}{r}\phi_{\sigma r} + \frac{1}{r^2}\phi_{\sigma\theta\theta} = \sigma M_\infty^2(2ik\phi_{\sigma x} - k^2\phi_\sigma) \tag{2}$$

where $\sigma = 0$ for the mean flow and $\sigma = 1$ for the unsteady flow and M_∞ is the freestream Mach number.

The boundary conditions are that no perturbation propagates ahead of the Mach wave surface emanating from the body apex and that the flow is tangent to the body surface. The latter condition can be expressed, in the body-fixed system, as

$$\frac{\partial\phi_\sigma}{\partial n} = B_\sigma \qquad \text{at } r = R(x,\theta) \tag{3}$$

where $\boldsymbol{n}$ is the outward normal to the body, for the steady mean flow ($\sigma = 0$), $B_0 = R_x$, and for the unsteady flow ($\sigma = 1$), $B_1 = B_1(R, R_x, R_\theta, g, g', g'', \phi_{0x}; k)$

The exact isentropic pressure coefficient C_p can be expanded to yield the linearized form in δ_0, i.e.:

$$C_p = C_p^0 + \delta_0 e^{ikt} C_p^1 \qquad \text{at } r = R(x,\theta) \tag{4}$$

where

$$C_p^0 = \frac{2}{\gamma M_\infty^2}[S_0^\gamma - 1] \text{ for the mean flow}$$

$$C_p^1 = -2\,S_0 J_1 \text{ for the unsteady flow}$$

$$S_0 = \left[1 - \frac{\gamma-1}{2}M_\infty^2\left(2\phi_{0x} + \phi_{0x}^2 + \phi_{0r}^2 + \frac{1}{R^2}\phi_{0\theta}^2\right)\right]^{\frac{1}{\gamma-1}}$$

γ is the specific heat ratio; and $J_1 = J_1(R, g, g', g'', \phi_{0x}, \phi_{0r}, \phi_{0\theta}, \phi_{1x}, \phi_{1r}, \phi_{1\theta}; k)$

Bundled Triplet Method

As mentioned earlier, using Fourier representation of an arbitrary body shape would introduce a formulation involving higher order kernel functions. In turn, the latter would yield an ill-condition AIC matrix. To circumvent this difficulty, the type of singularity distribution selected is preferred to remain low-order, i.e., sources and doublets. Then, if only the low-order singularities are employed, multiple lines of them have to be used to align with the body axis in order to represent an arbitrary body shape. This prompts the formulation of the present bundled triplet method.

As shown in Fig. 1, the body cross section is divided into M intervals. Each interval contains a finite sector $\Delta\Theta_m$, where $\Delta\Theta_m = \Theta_{m+1} - \Theta_m$, $m = 1,...M$, and $\Theta_1 = 0$, $\Theta_{m+1} = 2\pi$. A three-dimensional "pie" shape is defined by a portion of the body within the sector $\Delta\Theta_m$ whose vertex lies along the body axis. A line distribution of sources and another of doublets are superposed along the body axis for each pie segment. Within each pie segment an integral solution can be expressed (based on the superposition principle) as,

$$\phi_{1m}(x,r,\theta_m) = \int_0^{x-\beta r} F_m(\xi)\,B(x-\xi,\beta r)\,d\xi + \int_0^{x-\beta r} G_m(\xi)\frac{\partial}{\partial r}B(x-\xi,\beta r)\,d\xi\cdot\cos\Theta_m + \int_0^{x-\beta r} H_m(\xi)\frac{\partial}{\partial r}B(x-\xi,\beta r)\,d\xi\cdot\sin\Theta_m \tag{5}$$

where

$$B(x-\xi,\beta r) = e^{-i\mu(x-\xi)}\cdot\cos\lambda R_0/R_0$$

$$R_0 = [(x-\xi)^2\beta^2 r^2]^{1/2}$$

$$\mu = kM_\infty^2/\beta^2, \qquad \lambda = kM_\infty/\beta^2, \qquad \beta^2 = M_\infty^2 - 1$$

and $F_m(\xi)$ is the source strength solution, whereas $G_m(\xi)$ and $H_m(\xi)$ are two doublet strength solutions. It is clear now that our triplet model is a "generalized triplet," in that the singularity strength functions are different from each other. In the case of $F_m = G_m = H_m$, the generalized triplet model then reduces to the regular triplet model.[17] Furthermore, along the body axis, each of the triplet lines is discretized by N segments where $\Delta\xi_{j,m} = \xi_{j+1,m} - \xi_{j,m}$ for a given pie sector $\Delta\Theta_m$.

Harmonic Gradient Model

To achieve computation accuracy and effectiveness in the high-reduced frequency k and/or the low Mach number M_∞ domains, it is essential to render the doublet solution uniformly valid in the complete k and M_∞ domains. This can be simply achieved by modeling the doublet solution to maintain spatially harmonic in the mean flow direction. In so doing, the panel size $\Delta\xi_j$ is regulated and is made compatible to the wave number generated by the body oscillation. This is known as the H-G model introduced in Refs. 6 and 7.

Here, the H-G model employed for wings[6] and for axisymmetric bodies[7] is adopted to combine with the Bundled Triplet solutions. Application of the H-G model to Eq. (3) amounts to stating that in the interval $\xi_{j,m} \le \xi \le \xi_{j+1,m}$

$$F_m(\xi) = a_{j,m}(1 - e^{-i\mu\xi}) \tag{6a}$$

for the source solution, and

$$G_m(\xi) = (b_{j,m}\xi + d_{j,m})e^{-i\mu\xi} \tag{6b}$$

$$H_m(\xi) = (c_{j,m}\xi + h_{j,m})e^{-i\mu\xi} \tag{6c}$$

for the doublet solutions.

Note that Eqs. (6b) and (6c) are the direct application of the H-G model, whereas Eq. (6a) is a new extension of the H-G model to the source solution. It can be shown that both constants $d_{j,m}$ and $h_{j,m}$ can be expressed in terms of $b_{j,m}$ and $c_{j,m}$, respectively, when a continuity condition in G_m and H_m is imposed between the adjacent segments. Introducing Eqs.

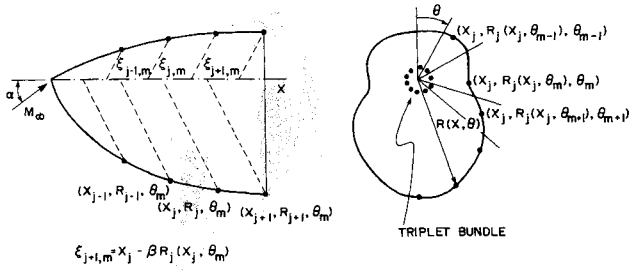

Fig. 1 Sketch showing bundled triplet arrangements.

(6a-c) and further discretization of the kernel integrals of Eq. (5) results in

$$\phi_1(P_i) = \sum_{j=1}^{i} a_{j,m} S_j^{j+1} + (b_{j,m}\cos\Theta_m + c_{j,m}\sin\Theta_m) D_j^{j+1} \quad (7)$$

Equation (7) represents the potential at a field point P_i, which lies within the domain of influence due to a part of the triplet line.

The domain of influence is defined by a pie segment bounded by the sector $\Delta\Theta_m$ and the inversed Mach cone intersection with respect to P_i. Hence, the effective triplet line is confined to the part from the body apex to the ith segment, where the discretized kernel integrals S_j^{j+1} and D_j^{j+1} represent the induced potential per unit source and doublet strengths respectively by the jth segment of the triplet line.

Least Square Procedure

For convenience, a surface panel is defined as a body surface element whose area is bounded by $R \cdot \Delta\Theta_m$ and $\Delta\xi_j$. A control point is located at $(x_i, R_i(x_i, \bar{\Theta}_m), \bar{\Theta}_m)$, the central point of each panel, where $i = 1,...N$, $m = 1,...M$, and $\bar{\Theta}_m = (\Theta_m + \Theta_{m+1})/2$. To obtain the potential values of $\phi_{i,m}$ at the control point, one effective way is to relate the unknowns $a_{j,m}$, $b_{j,m}$, and $c_{j,m}$ to the crossflow potential $\phi_{i,m}$ by means of the method of weighted least squares. (For simplicity, we have dropped the subscript "1" in $\phi_{1i,m}$, hereafter.) Thus, a weighted integral is established, whose discretized form can be expressed as

$$I = \frac{1}{2}\sum_{h=m-1}^{m+1} W_h \left\{ \left[\sum_{j=1}^{i} a_{j,m} S_j^{j+1} + (b_{j,m}\cos\Theta_h + c_{j,m}\sin\Theta_h) D_j^{j+1} \right] - \phi_{i,h} \right\}^2 \quad (8)$$

where S_j^{j+1} and D_j^{j+1} are now evaluated at the control point $(x_i, R_i(x_i, \bar{\Theta}_h)\ \bar{\Theta}_h)$; $\phi_{i,h}$ represents the exact value of the potential at the ith point, and W_h is the introduced weight function. Note that Eq. (8) is a least square procedure set up for three adjacent panels, namely from $(m-1)$ to $(m+1)$. Thus, by imposing

$$\frac{\partial I}{\partial a_{i,m}} = \frac{\partial I}{\partial b_{i,m}} = \frac{\partial I}{\partial c_{i,m}} = 0$$

we can now relate the unknowns $a_{i,m}$, $b_{i,m}$, and $c_{i,m}$ to $\phi_{i,m-1}$, $\phi_{i,m}$, and $\phi_{i,m+1}$ by a least square matrix $[LS]$, i.e.,

$$\begin{Bmatrix} a_{i,m} \\ b_{i,m} \\ c_{i,m} \end{Bmatrix} = [LS]\{\phi_{i,m}\} \quad (9)$$

for $i = 1,...N$ and $m = 1,...M$. On the LHS of Eq. (9), the column vector has the dimension of $(3 \times N \times M)$, whereas on the RHS, $[LS]$ is a matrix of dimension $(3 \times N \times M) \times (N \times M)$, and the unknown potential $\phi_{i,m}$ is a column vector of dimension $(N \times M)$.

Hence, the velocities at the control point can be expressed as

$$\left\{\frac{\partial\phi}{\partial x_i}\right\} = [U][LS]\{\phi_{i,m}\} \quad (10a)$$

$$\left\{\frac{\partial\phi}{\partial r_i}\right\} = [V][LS]\{\phi_{i,m}\} \quad (10b)$$

$$\left\{\frac{1}{r_i}\frac{\partial\phi}{\partial\theta_m}\right\} = [W][LS]\{\phi_{i,m}\} \quad (10c)$$

where $[U]$, $[V]$ and $[W]$ are matrices of dimension $(N \times M) \times (3 \times N \times M)$, containing the velocity influence coefficients in the x, r and θ direction. Now, the velocities

$$\frac{\partial\phi}{\partial x_i},\ \frac{\partial\phi}{\partial r_i},\ \frac{1}{r_i}\frac{\partial\phi}{\partial\theta_m}$$

in the tangency condition [Eq. (3)] can be replaced by the crossflow potential $\phi_{i,m}$ through Eq. (10). Consequently, $\{\phi_{i,m}\}$ is the unknown to be solved in Eq. (3).

In passing, we note that the evaluation of the steady mean flow potential follows the same procedure as described above, except that the kernel integrals S_j^{j+1} and D_j^{j+1} are to be replaced by their steady counterparts.

Body-wing Combinations

For oscillating thin wings in supersonic flow, the perturbed potential solution can be expressed as

$$\phi_1(x,y,z) = \int\int_A \Delta C_p\, e^{-i\mu(x-\xi)} \left[\frac{\partial}{\partial\zeta} \int^{\xi} \frac{\cos(\lambda\bar{R})}{\bar{R}}\, e^{-i\mu(x-\nu)} d\nu \right] dA \quad (11)$$

where

$$\bar{R}^2 = (x-\nu)^2 - \beta^2[(y-\eta)^2 + (z-\zeta)^2],$$

$$\Delta C_p = C_p^{\ell} - C_p^{u}$$

and A is the effective wing area intersected by the inversed Mach cone originated from the point (x,y,z).

The above integral solution is obtained based on the acceleration potential assumption, i.e., $\Delta C_p \simeq -2(\Delta\phi_{1x} + ik\Delta\phi_1)$. It should be pointed out that, in terms of body-wing interaction, this assumption amounts to neglecting the coupling terms such as $\phi_{0x}\Delta\phi_{1x}$, $\phi_{0y}\Delta\phi_{1y}$, $\phi_{0z}\Delta\phi_{1z}$ in the pressure coefficient.

The interference between the body and the wing is provided by the tangency condition. In terms of the matrix form, the tangency condition can be expressed as

$$\begin{bmatrix} \left(\frac{\partial\phi}{\partial n}\right)_{BB} & \left(\frac{\partial\phi}{\partial n}\right)_{BW} \\ \left(\frac{\partial\phi}{\partial n}\right)_{WB} & \left(\frac{\partial\phi}{\partial n}\right)_{WW} \end{bmatrix} \begin{Bmatrix} \phi_B \\ \Delta C_{pW} \end{Bmatrix} = \begin{Bmatrix} B_B \\ B_W \end{Bmatrix} \quad (12)$$

where $(\partial\phi/\partial n)_{BB}$ represents the normal velocity influence coefficient induced by the body onto itself, $(\partial\phi/\partial n)_{WB}$ the body on the wing, $(\partial\phi/\partial n)_{BW}$ the wing on the body, and $(\partial\phi/\partial n)_{WW}$ the wing onto itself; B_B and B_W are the downwash velocities on the body surface and on the wing surface, respectively; ΔC_{pW} denotes the pressure on the wing. Equation (12) is solved to yield ΔC_{pW}. The velocities on the body can be evaluated at the control points from Eqs. (10a-c). Consequently, the pressure on the body can be determined from Eq. (4).

The generalized forces Q_{IJ} can be expressed in terms of the unsteady pressure coefficient C_p^1 and of the mode shape g as

$$Q_{IJ} = \frac{1}{S_{\text{ref}}} \int\int_S C_p^{1(J)} (n_x g'^{(I)} z - g^{(I)} n_z)\, ds \quad (13)$$

where S is the wing plus the body surface area; n_x and n_z are the normal components in the x and z direction to the wing and body surfaces, respectively; z is the ordinate of the control point; $C_p^{1(J)}$ is the unsteady pressure coefficient due to the Jth mode; $g^{(I)}$ is the Ith mode of oscillation, and S_{ref} represents the maximum area or the based area for the body-alone cases, or it represents the wing planform area for the wing-body combination cases.

The stability derivatives are related to the generalized forces by the following formulas:

$$C_{L_\alpha} = R_e(Q_{12})$$

$$C_{m_\alpha} = \frac{R_e(Q_{22})}{L}$$

$$C_{N_{\dot\alpha}} + C_{Nq} = \frac{I_m(Q_{12})}{k}$$

$$C_{m_{\dot\alpha}} + C_{mq} = \frac{I_m(Q_{22})}{kL} \tag{14}$$

where L is the body length for body alone cases, and the wing mean chord for body-wing combination cases; k is the reduced frequency based on L. Q_{12} and Q_{22} are the 12 and 22 components of the generalized force matrix representing two rigid-body modes. The former one is the plunging mode and the latter the pitching mode.

Panel Flutter

An interesting application of the present method is to study the supersonic panel flutter problem for cylindrical shells. Previously, Dowell and Widnall[18] used Laplace transform technique to study this problem, whereas Platzer et al.[19] used the Linearized Method of Characteristics (LMOC). The objective of these studies is to evaluate the generalized forces acting on the vibrating cylindrical panel of an otherwise rigid, infinitely long, cylindrical shell.

Let L be the length of the cylindrical panel, i.e., $0 \le x \le L$. Along the cylindrical shell, the oncoming flow upstream of the panel is uniformly supersonic. The cylindrical panel is allowed to perform small-amplitude harmonic oscillations (see Fig. 6).

For inviscid analysis of panel flutter, Eq. (2) ($\sigma = 1$) is the commonly used governing equation. On the mean surface of the cylindrical panel, $r = R$, the tangency condition reads:

$$\phi_{1r} = ikh + h_x \qquad 0 \le x \le L$$

$$= 0 \qquad x < 0 \tag{15}$$

where h is the mode shape of the vibrating panel, defined as

$$h(x, \Theta) = \sin(j\pi x)\cos(n\theta) \tag{16}$$

The unsteady pressure coefficient C_p^1 on the panel surface is simply

$$C_p^1 = -2[\phi_{1x} + ik\phi_1] \tag{17}$$

and the generalized aerodynamic forces Q_{ij} read

$$Q_{ij} = \frac{1}{2C}\int_0^{2\pi}\int_0^L C_p^{1(i)} \sin(j\pi x)\cos(n\theta) R\, d\theta\, dx \tag{18}$$

where $C_p^{1(i)}$ is the unsteady aerodynamic pressure, due to the mode $\sin(i\pi x)\cos(n\theta)$ and $C = 2\pi$ for $n = 0$ and π for $n \neq 0$.

Bundled triplets are placed along the x-axis in the interval $-\beta R < \xi < L - \beta R$. The panel elements and control points between $0 \le x \le L$ and $0 \le \Theta \le 2\pi$ on the mean surface are distributed according to the cosine law in both x and Θ directions. Combining Eqs. (10b), (15), and (16) results in the following tangency condition evaluated at the control points.

$$[V][LS]\{\phi_{i,m}\} = \{[ik\sin(j\pi x_i) + j\pi\cos(j\pi x_i)]\cos(n\Theta_m)\} \tag{19}$$

The potential values $\phi_{i,m}$ can now be obtained from the above equation. Thus, the unsteady pressure and the generalized forces can be evaluated according to Eqs. (17) and (18).

In the present formulation, the circumferential mode shape [i.e., the $\cos(n\Theta)$ factor] is retained throughout the analysis, whereas in Refs. 18 and 19, $\cos(n\Theta)$ is factorized out in their formulation. As a result, the number of control points required in the circumferential direction increases rapidly with an increase in n, although the computation time is still comparatively rapid. It is essential to point out that the present method is a full three-dimensional one, which can treat a much wider scope of problems than those in Refs. 18 and 19. Feasible applications in panel flutter using the present method include closed (pointed) bodies of circular or noncircular cross sections and vibrating panels of nonharmonic mode shapes (i.e., the case of partially oscillating shells).

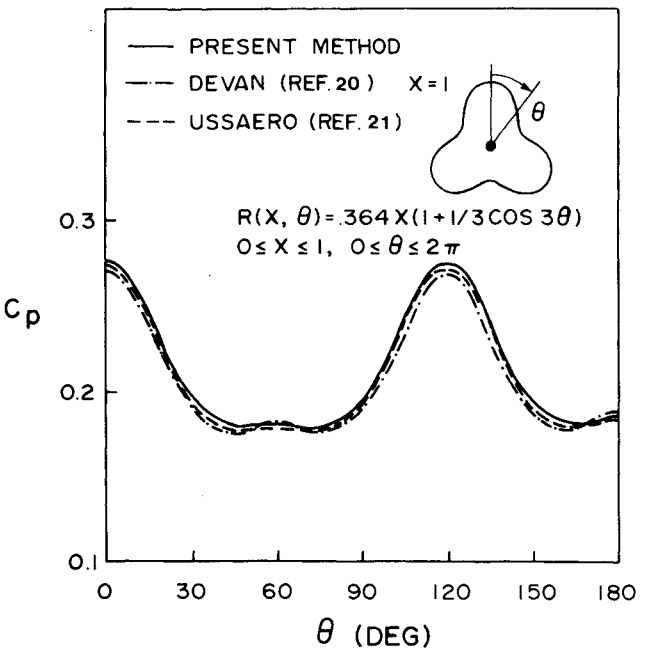

Fig. 2 Steady pressure distributions for an asymmetric cone at $M_\infty = 2.0$ and angle of attack $\alpha = 0$ deg.

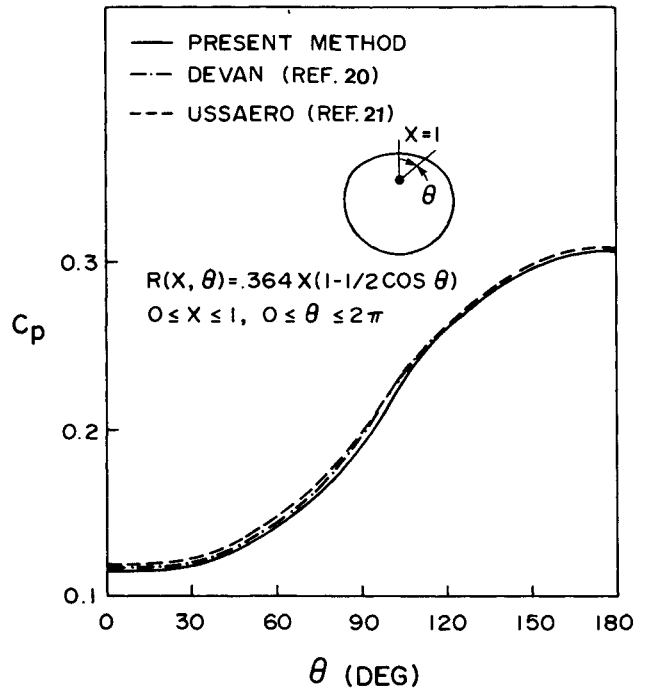

Fig. 3 Steady pressure distributions for asymmetric cone at $M_\infty = 2.0$ and angle of attack $\alpha = 0$ deg.

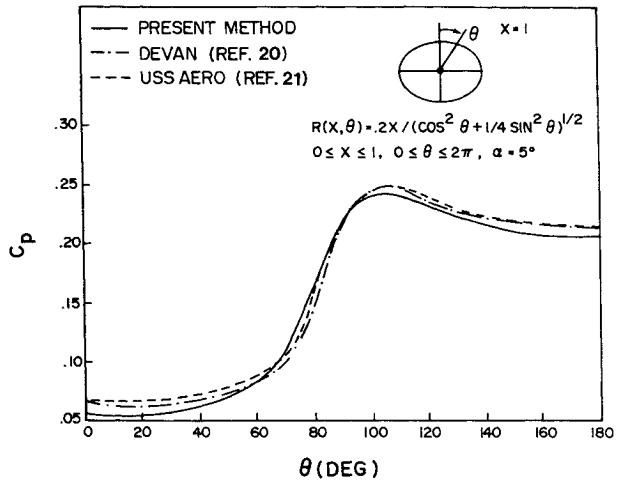

Fig. 4 Steady pressure distributions for an elliptic cone at $M_\infty = 2.0$ and angle of attack $\alpha = 5$ deg.

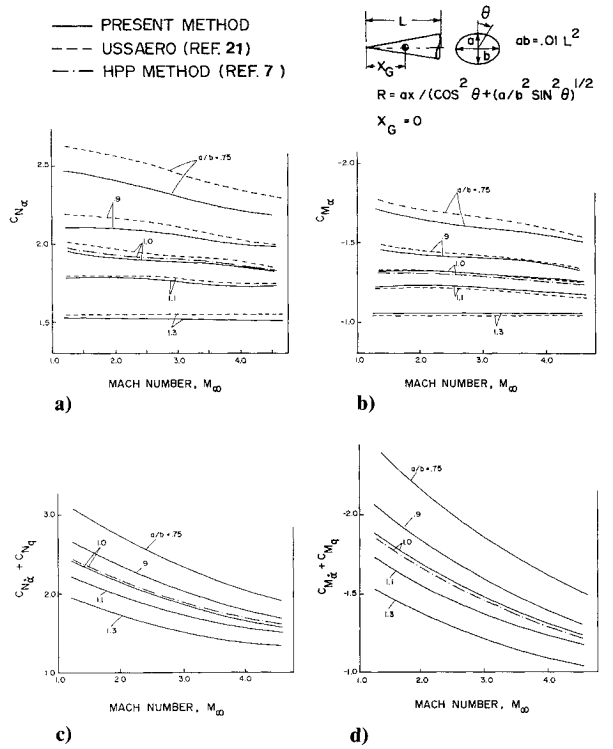

Fig. 5 Stability derivatives of a family of elliptic cones at various Mach numbers: a) Normal force derivatives; b) pitch moment derivatives; c) damping normal force derivatives; and d) damping moment derivatives.

Results and Discussion

To validate the present method, numerical examples in terms of steady pressures, stability derivatives, and generalized forces are presented for asymmetric bodies, cylindrical panels, and wing-body combinations.

Asymmetric Bodies

The steady pressure distributions for three different asymmetric conical bodies are presented in Figs. 2, 3, and 4 at the same freestream Mach number $M_\infty = 2.0$. Since the flowfields are conical, only the circumferential C_p is presented for these cases. Asymmetric configurations as shown in Figs. 2 and 3 are placed at mean angle of attack $\alpha = 0$, whereas the elliptic cone in Fig. 4 is at $\alpha = 5$ deg. Since the flow is symmetrical with respect to the meridian plane, pressures on half of the body are presented ($0 \le \Theta \le 180$ deg). Because of the steeper variation in the given body curvature (due to cos 3Θ), a bundle of 36 triplet lines is distributed in equal circumferential intervals for a full body in Fig. 2. The geometries in Figs. 3 and 4 are less complicated; only 18 triplet lines were used for full bodies in both cases. It can be seen that the present computed results are in good agreement with Devan's results, using the finite difference method[20] and the USSAERO results.[21] Typically, we use 40 panels in the circumferential direction in the USSAERO program for obtaining results in Figs. 2, 3, and 4. In the present method, 5 segments are used in the x direction. This amounts to a total of 100 ~ 200 panels and control points to be evaluated. Because the evaluation scheme of the present kernel is much simpler, the CPU time required is about one-tenth of that needed in the USSAERO code.

Figure 5 presents the static (Figs. 5a, 5b) and dynamic (Figs. 5c, 5d) normal force and moment coefficients at various Mach numbers for a family of elliptic cones placed at zero mean angle of attack. The ellipticity ratio, as defined by a/b, ranges from 0.75 to 1.3. Figures 5a and 5b compare the present results with those computed by USSAERO. There appears to be an increase in discrepancies as the elliptic cone becomes

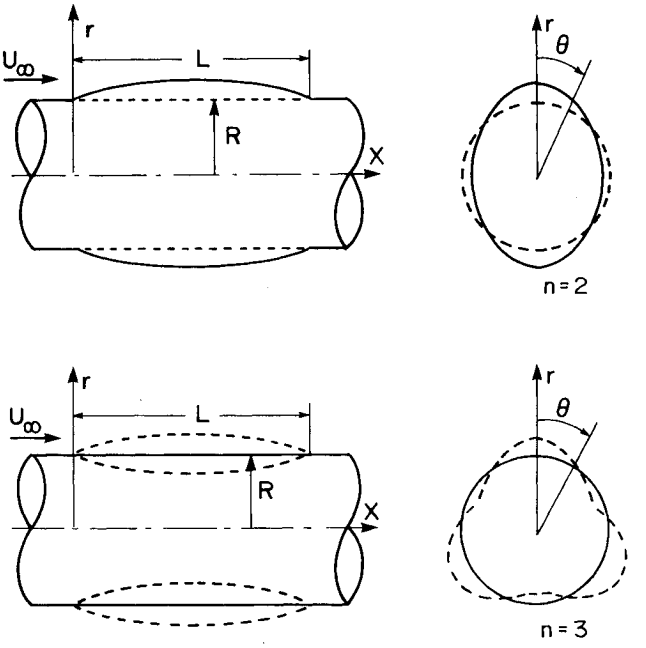

Fig. 6 Cylindrical flutter showing two vibrating modes.

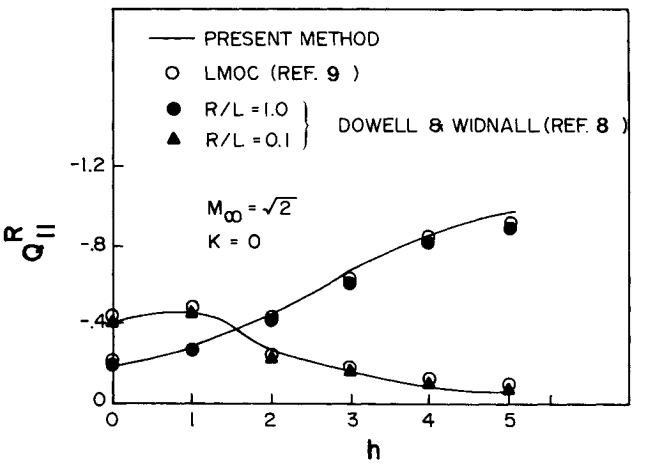

Fig. 7 Real part of the generalized aerodynamic force Q_{11} vs circumferential mode number.

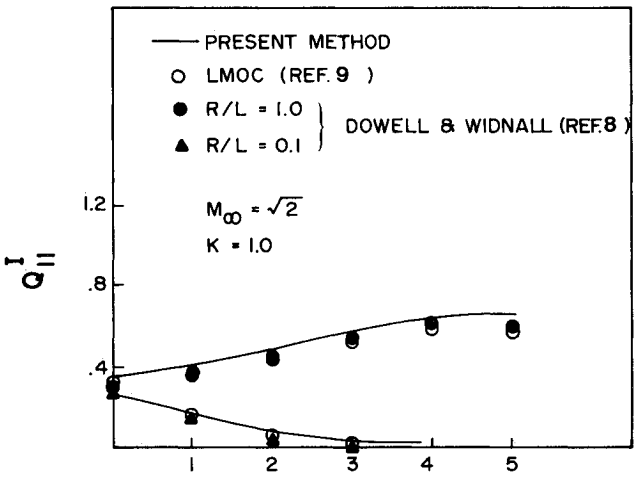

Fig. 8 Imaginary part of the generalized aerodynamic force Q_{11} vs circumferential mode number.

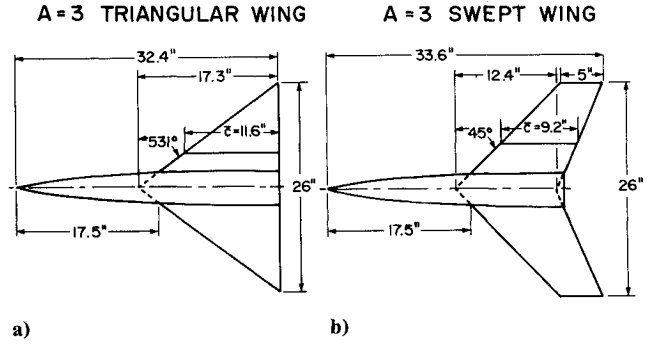

Fig. 9 Sketches of wing-body configurations: a) Aspect ratio $\mathcal{R}=3$ triangular wing-body; and b) aspect ratio $\mathcal{R}=3$ swept wing-body.

more wing-like, i.e., $a/b > 1$. When the ratio approaches one, all results converge to the results for a circular cone, as obtained by Garcia-Fogeda and Liu.[7]

Similarly, the computed results for the out-of-phase normal forces and moment coefficients (Figs. 5c and 5d) also converge to those obtained in Ref. 7, when a/b approaches one as expected. In passing, we note that little Mach dependency is observed for the static moments (about $x_G = 0$), whereas the damping moment decreases rapidly with increasing Mach number. Furthermore, all results confirm the expected trend that both the static and the damping moments increase with decreasing ellipticity ratio, i.e., as the body becomes more wing-like.

Cylindrical Panel Flutter

In order to validate the present method in the high-frequency domain, supersonic cylindrical flutter cases (Fig. 6) are selected for comparison with existing theories.[18,19]

A bundle of triplet lines are arranged according to a cosine distribution, both in the circumferential and in the axial directions ($0 \le \Theta \le 2\pi$ and $0 \le x \le 1$). The cylindrical panel is first evenly divided into n intervals in the circumferential direction, say $n = 5$. Within each interval, eight control points are used, given a total of 40 control points. In the axial direction, 25 points are used for all n intervals.

The real and the imaginary part of the generalized forces on the cylindrical panel are presented in Figs. 7 and 8 for the freestream Mach number $M_\infty = \sqrt{2}$ and the reduced frequencies $k = 0$ and 1.0. The generalized forces are computed based on Eq. (13).

It is seen that good agreements are found between the present results and those of Dowell and Widnall[18] and of Platzer et al.[19] up to $n = 5$ for both reduced frequencies ($k = 0$ and 1.0).

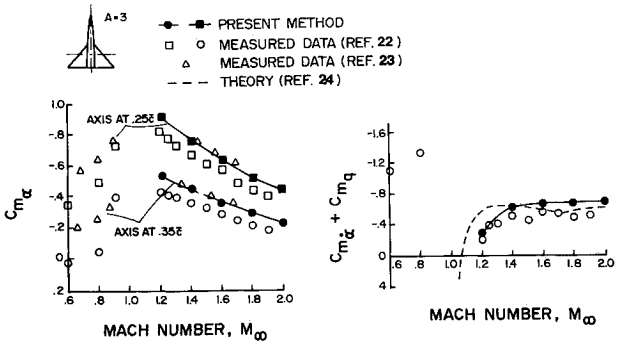

Fig. 10 Static and dynamic moment derivatives for an aspect ratio $\mathcal{R} = 3$ triangular wing-body.

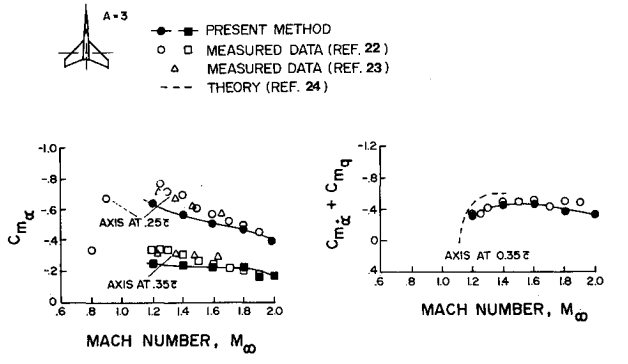

Fig. 11 Static and dynamic moment derivatives for an aspect ratio $\mathcal{R} = 3$ swept wing-body.

Wing-body Combinations

To verify the present results for wing-body combinations in the low-frequency limit, measured stability derivatives in Refs. 22 and 23 are selected for comparison. Two configurations are selected, as shown in Fig. 9:

Case A: Aspect ratio $\mathcal{R} = 3.0$, triangular wing-body
Case B: Aspect ratio $\mathcal{R} = 3.0$, swept wing-body

To compute the stability derivatives for these configurations, a bundle of 20 triplet lines is used for the body. With 10 segments along the body axis, this amounts to 200 control points on the body surface. However, only 50 panels are required for modeling the wings.

Figures 10 and 11 show the computed static and damping moments for the wing-body configurations in cases A and B, respectively. Good agreements are found between the present results and the measured data in the overall Mach number ranges at two pitching-axis locations, $x_G = 0.25\bar{c}$ and $0.35\bar{c}$ ($\bar{c}$ is the chord length). For damping moment calculations, one notices that the predicted results of the analytical theory[24] deviate further from the measured data than the present results. This is due to the fact that an analytical solution of a rectangular wing is used to approximate that of delta and swept wing planforms.

Conclusion

A new supersonic method has been developed to compute the unsteady aerodynamics for arbitrary bodies and wing-body combinations. The method extends the Harmonic-Gradient (H-G) model to our recently developed Bundled Triplet Method (BTM) in order to properly account for the unsteady wing-body interference. It has been shown that the present method has the following features:

1) With the H-G model, the BTM is computationally efficient and robust for unsteady flow computations in the full-frequency range.

2) Although the total number of panels needed for BTM is comparable to that of a surface panel method, the CPU time is only one-tenth of the latter.

3) The BTM places the control points on the exact body surface, whereas a surface panel method usually places the control points on the approximate surface.

To validate the present method, numerical examples have been studied for various three-dimensional configurations. These include steady pressures on three asymmetric conical bodies, generalized forces for cylindrical panel flutter, and stability derivatives for bodies and wing-body combinations. It is found that all computed results are in good agreement with existing theoretical results and measured data.

Acknowledgment

The present work is supported in part by the U.S. Army Research Office, Durham, N.C. The contract is monitored by Drs. Robert E. Singleton and Thomas L. Doligalski.

References

[1]Jones, W. P. and Appa, K., "Unsteady Supersonic Aerodynamics Theory for Interfering Surfaces by the Method of Potential Gradient," NASA CR-2898, Oct. 1977.

[2]Hounjet, M. H. L., "An Improved Potential Gradient Method to Calculate Airloads on Oscillating Supersonic Interfering Surfaces," *Journal of Aircraft,* Vol. 19, No. 5, 1982, pp. 390–399.

[3]Ueda, T. and Dowell, E. H., "Doublet-Point Method for Supersonic Unsteady Lifting Surfaces," *AIAA Journal,* Vol. 22, Feb. 1984, pp. 179–186.

[4]Lottati, I. and Nissim, E., "Nonplanar Supersonic Three-Dimensional Oscillatory Piecewise Continuous Kernel-Function Method," *Journal of Aircraft,* Vol. 24, Jan. 1987.

[5]Appa, K., "Constant Pressure Panel Method for Supersonic Unsteady Airload Analysis," *Journal of Aircraft,* Vol. 24, Oct. 1987, pp. 696–702.

[6]Chen, P. C. and Liu, D. D., "A Harmonic Gradient Method for Unsteady Supersonic Flow Calculations," *Journal of Aircraft,* Vol. 22, May 1985, pp. 371–379.

[7]Garcia-Fogeda, P. and Liu, D. D., "Analysis of Unsteady Aerodynamics for Elastic Bodies in Supersonic Flow," *Journal of Aircraft,* Vol. 24, No. 12, 1987, pp. 833–840; also AIAA Paper 86-007, 1986.

[8]Garcia-Fogeda, P. and Liu, D. D., "Aeroelastic Application of Harmonic Potential Panel Method to Oscillating Flexible Bodies in Supersonic Flow," AIAA Paper 86-0864-CP, 1986; also *Journal of Spacecraft and Rockets,* Vol. 25, No. 4, 1988, pp. 271–277.

[9]Liu, D. D., Garcia-Fogeda, P., and Chen, P. C., "Oscillating Wings and Bodies with Flexure in Supersonic Flow—Application of Harmonic Potential Panel Method," International Council of the Aeronautical Sciences paper 86-2.9.4, 1986; also *Journal of Aircraft,* Vol. 25, No. 6, 1988, pp. 507–514.

[10]Wards, G. N., *Linearized Theory of Steady High-Speed Flow, Part III, Slender Body Theory,* University Press, Cambridge, England, 1955.

[11]Nielsen, J. N., "Quasi-cylindrical Theory of Wing-Body Interference at Supersonic Speeds and Comparison with Experiment," NACA Report 1252, 1955.

[12]Woodward, F. A., "Analysis and Design of Wing-Body Combinations at Subsonic and Supersonic Speeds," *Journal of Aircraft,* Vol. 5, No. 6, Nov.–Dec. 1968, pp. 528–534.

[13]Garcia-Fogeda, P. and Liu, D. D., "Three Dimensional Analysis of Supersonic Flows Around Arbitrary Bodies Using Boundary Collocation Method," *Boundary Element Techniques: Applications in Fluid and Computational Aspects,* edited by C. A. Brebbia and W. S. Venturini, Computational Mechanics Publications, 1987, pp. 75–87.

[14]von Karman, T., "Calculation of Pressure Distributions on Airship Hulls," NACA TM 574, 1930.

[15]von Karman, T. and Moore, N. B., "The Resistance of Slender Bodies," Trans. American Society of Mechanical Engineers 54-27, 1932, pp. 303–310.

[16]Morino, L., Chen, L. T., and Suciu, E. O., "Steady and Oscillating Subsonic and Supersonic Aerodynamics Around Complex Configuration," *AIAA Journal,* Vol. 13, Mar. 1975.

[17]Woodward, F. A. and Landrum, E. J., "The Supersonic Triplet—A New Aerodynamic Panel Singularity with Directional Properties," *AIAA Journal,* Vol. 18, Feb. 1980.

[18]Dowell, E. H. and Widnall, S. E., "Generalized Aerodynamic Forces on an Oscillating Cylindrical Shell," *Quarterly of Applied Mathematics,* No. 1, 1966, pp. 1–17.

[19]Platzer, M. F., Brix C. W., Jr., and Webster, K. A., "Linearized Characteristics Method for Supersonic Flow Past Vibrating Shells," *AIAA Journal,* Vol. 11, No. 9, 1973, pp. 1302–1305.

[20]Devan, L., "Conical, Noncircular, Second-Order Potential Theory of Supersonic Flow," *AIAA Journal,* Vol. 22, No. 5, 1984, pp. 618–623.

[21]Woodward, F. A., "An Improved Method for the Aerodynamic Analysis of Wing-Body-Tail Configurations in Subsonic and Supersonic Flow," NASA CR-2228, 1973.

[22]Tobak, M., "Damping-in-Pitch of Low-Aspect-Ratio Wings at Subsonic and Supersonic Speeds," NACA RM A52L04a, 1953.

[23]Heitmeyer, J. C., "Lift, Drag, and Pitching Moment of Low-Aspect-Ratio Wings at Subsonic and Supersonic Speeds—Plane Triangular Wing of Aspect Ratio 3 with NACA 0003-63 Sections," NACA RM A51H02, 1951.

[24]Henderson, A. Jr., "Pitching-Moment Derivatives C_{mq} and $C_{.\alpha}$ at Supersonic Speeds for a Slender-Delta-Wing and Slender-Body Configuration and Approximate Solutions for Broad-Delta-Wing and Slender-Body Combinations," NACA TNL553, 1951.